Remote Sensing of Environment 112 (2008) 3234–3247

Contents lists available at ScienceDirect

Remote Sensing of Environment

journal homepage: www.elsevier.com/locate/rse

Leaf chlorophyll content retrieval from airborne hyperspectral remote sensing imagery

Yongqin Zhang [a,*], Jing M. Chen [a], John R. Miller [b], Thomas L. Noland [c]

[a] University of Toronto, 100 St. George St., Room 5047, Toronto, Ont., Canada M5S 3G3
[b] York University, 4700 Keele Street, Toronto, Ont., Canada M3J 1P3
[c] Ontario Forest Research Institute, 1235 Queen St. East, Sault Ste. Marie, ON, Canada P6A 2E5

ARTICLE INFO

Article history:
Received 9 February 2007
Received in revised form 31 March 2008
Accepted 5 April 2008

Keywords:
Leaf chlorophyll content
Retrieval
Hyperspectral remote sensing
CASI
Canopy structure
Geometrical–Optical model
Look-up-table approach

ABSTRACT

Hyperspectral remote sensing has great potential for accurate retrieval of forest biochemical parameters. In this paper, a hyperspectral remote sensing algorithm is developed to retrieve total leaf chlorophyll content for both open spruce and closed forests, and tested for open forest canopies. Ten black spruce (*Picea mariana* (Mill.)) stands near Sudbury, Ontario, Canada, were selected as study sites, where extensive field and laboratory measurements were carried out to collect forest structural parameters, needle and forest background optical properties, and needle biophysical parameters and biochemical contents chlorophyll *a* and *b*. Airborne hyperspectral remote sensing imagery was acquired, within one week of ground measurements, by the Compact Airborne Spectrographic Imager (CASI) in a *hyperspectral mode*, with 72 bands and half bandwidth 4.25–4.36 nm in the visible and near-infrared region and a 2 m spatial resolution. The geometrical–optical model 4-Scale and the modified leaf optical model PROSPECT were combined to estimate leaf chlorophyll content from the CASI imagery. Forest canopy reflectance was first estimated with the measured leaf reflectance and transmittance spectra, forest background reflectance, CASI acquisition parameters, and a set of stand parameters as inputs to 4-Scale. The estimated canopy reflectance agrees well with the CASI measured reflectance in the chlorophyll absorption sensitive regions, with discrepancies of 0.06%–1.07% and 0.36%–1.63%, respectively, in the average reflectances of the red and red-edge region. A look-up-table approach was developed to provide the probabilities of viewing the sunlit foliage and background, and to determine a spectral multiple scattering factor as functions of leaf area index, view zenith angle, and solar zenith angle. With the look-up tables, the 4-Scale model was inverted to estimate leaf reflectance spectra from hyperspectral remote sensing imagery. Good agreements were obtained between the inverted and measured leaf reflectance spectra across the visible and near-infrared region, with $R^2=0.89$ to $R^2=0.97$ and discrepancies of 0.02%–3.63% and 0.24%–7.88% in the average red and red-edge reflectances, respectively. Leaf chlorophyll content was estimated from the retrieved leaf reflectance spectra using the modified PROSPECT inversion model, with $R^2=0.47$, RMSE = 4.34 μg/cm^2, and jackknifed RMSE of 5.69 μg/cm^2 for needle chlorophyll content ranging from 24.9 μg/cm^2 to 37.6 μg/cm^2. The estimates were also assessed at leaf and canopy scales using chlorophyll spectral indices TCARI/OSAVI and MTCI. An empirical relationship of simple ratio derived from the CASI imagery to the ground-measured leaf area index was developed ($R^2=0.88$) to map leaf area index. Canopy chlorophyll content per unit ground surface area was then estimated, based on the spatial distributions of leaf chlorophyll content per unit leaf area and the leaf area index.

1. Introduction

Monitoring forest health and stress from remotely sensed images is of concern for forest management. Spectrally continuous hyperspectral remote sensing data can provide information on forest biochemical contents, which are important for studying vegetation stress, nutrient cycling, productivity, and species recognition etc. (Asner et al., 1998; Curran, 1994; Davidson et al., 1999; Lewis et al., 2001; Noland et al., 2003; Sampson et al., 2003; Zarco-Tejada et al., 2004a,b). Healthy and stressed vegetations present different reflectance features in the green peak and along the red-edge due to changes in pigment levels (Belanger et al., 1995; Carter, 1994; Gitelson et al., 1996; Rock et al., 1988). Leaf chlorophyll content is the main parameter determining leaf spectral variation in the visible regions. Quantitative estimates of leaf chlorophyll content from hyperspectral data can provide a useful means for assessing forest growth and stress as affected by insects and diseases (Sampson et al., 2003). Total leaf chlorophyll content, and the ratio of chlorophyll *a* to *b* decrease when

* Corresponding author. Tel.: +1 416 978 7085; fax: +1 416 946 7715.
E-mail addresses: zhangy@geog.utoronto.ca (Y. Zhang), chenj@geog.utoronto.ca (J.M. Chen), jrmiller@yorku.ca (J.R. Miller), tom.noland@mnr.gov.on.ca (T.L. Noland).

0034-4257/$ – see front matter © 2008 Elsevier Inc. All rights reserved.
doi:10.1016/j.rse.2008.04.005

vegetation is under stress (Fang et al., 1998). The dependence of spectra on leaf biochemical properties provides the physical bases for remote detection of vegetation stresses through monitoring the change of chlorophyll content. Hyperspectral remote sensing with high spatial resolution has been demonstrated to be useful for detecting tree stress due to insect attack (Lawrence & Labus, 2003).

Empirical relationships between spectral indices and chlorophyll content measurements have been exploited for estimating leaf chlorophyll content. At the leaf level, optical indices have been widely used for plant species discrimination (Belanger et al., 1995), leaf vigor evaluation (Luther & Carroll, 1999), vegetation stress assessment (Carter, 1994; Gitelson & Merzlyak, 1996; Rock et al., 1988), and leaf chlorophyll estimation (Datt, 1998, 1999). le Maire et al. (2004) summarizes the chlorophyll spectral indices published until 2002. Most spectral indices employ ratios of narrow bands within spectral ranges that are sensitive to chlorophylls to those not sensitive and/or related to some other controls on reflectance. This method solves the problem of overlapping absorption spectra of different pigments, the effects of leaf surface interactions, and leaf and canopy structure (Chappelle et al., 1992; Peñuelas et al., 1995). Though spectral indices provide non-destructive, efficient, and sensitive measurements of leaf pigment contents from leaf spectral reflectance, these optical indices are generally developed for a specific species. As the size, shape, surface, and internal structure of leaves may vary from species to species, the application of optical indices to other vegetation types or biomes needs to be re-investigated. Efforts have been made to improve the robustness and generality of chlorophyll indices by testing over a range of species and physiological conditions. Nevertheless, spectral indices need calibration when applied to a specific species.

Statistical estimation of canopy-level biochemical contents is performed through different methods. The simplest way is to directly develop statistical relationships between ground-measured biochemical contents and canopy reflectance measured in the field or by airborne or satellite sensors (Curran et al., 1997; Johnson et al., 1994; Matson et al., 1994; Zarco-Tejada & Miller, 1999). Alternatively, some leaf-level relationships between optical indices and pigment content are directly applied to the canopy-level estimation (Peterson et al., 1988; Yoder & Pettigrew-Crosby, 1995; Zagolski et al., 1996). Canopy biochemical composition depends strongly on plant species as well as on canopy structure. Confounding factors that influence the remotely sensed optical properties make it difficult to spatially and temporally extrapolate leaf-level relationships to canopy-level. From the leaf to the canopy scale, the complicated perturbations of canopy structure to light transfer need to be carefully considered. Statistical relationships are often site- and species-specific, and thus cannot be directly applied to other study sites since the canopy structure and viewing geometry may vary from different sites and species.

Considerable progress has been made in physically based modeling approaches to estimate leaf biochemical contents. At the leaf level, numerical inversion of leaf-level radiative transfer (RT) models, such as PROSPECT and LEAFMOD, have been used to predict leaf chlorophyll content (Demarez et al., 1999; Ganapol et al., 1998; Jacquemoud & Baret, 1990; Renzullo et al., 2006; Zarco-Tejada et al., 2001). Studies using coupled leaf and canopy RT models attempt to understand the effects of controlling factors on leaf reflectance properties at the canopy scale (Demarez & Gastellu-Etchegorry, 2000). Canopy reflectance models are used to scale up the leaf-level relationship between optical indices and pigment content (Zarco-Tejada et al., 2001). Canopy RT models or ray-tracing models are also coupled with leaf RT models for pigment content retrieval (Dawson et al., 1997; Demarez & Gastellu-Etchegorry, 2000; Jacquemoud et al., 1995; Moorthy et al., in press; Zarco-Tejada et al., 2004a,b). Coupled models refine the development of spectral indices, which are insensitive to factors such as canopy structure, illumination geometry, and background reflectance for estimating foliar chlorophyll concentrations from canopy reflectance (Broge & Leblanc, 2000; Daughtry et al., 2000).

Canopy RT models often assume that a canopy is composed of horizontal, homogeneous vegetation layers with infinite extent and Lambertian scatterers. Elements of the canopy are assumed to be randomly distributed in space as a turbid medium (Liang & Strahler, 1993; Verhoef, 1984; Verstaete et al., 1990). It is suitable for close and dense canopies such as corn, soybean, and grass canopies where the foliage spatial distribution is close to randomness. At the canopy scale, especially for the heterogeneous, open, and clumped forest canopies, canopy structural effects on remote sensing signals are considerable. As remote sensing signals originating from vegetated surfaces are determined by both canopy structure and leaf optical properties, the structural effects in open forests cannot be ignored. Canopy RT models do not consider canopy architecture, they are valid only for closed canopy with high LAI (LAI>3) (Zarco-Tejada, 2000). Efforts have been made to deal with canopy structural effects on the retrieval of forest biochemical parameters. Zarco-Tejada et al. (2001) estimate leaf chlorophyll content through coupled leaf and canopy-level RT models using the red-edge index as a merit function to minimize the effects of forest canopy structure, shadows, and openings. The application of the method was extended to coniferous forests for scaling leaf-level pigment estimation to canopy-level using high spatial resolution airborne imagery to select only bright-crown pixels in the scene for analysis (Moorthy et al., in press; Zarco-Tejada et al., 2004a). Though this method produces promising results for leaf chlorophyll content retrieval, the structural effects imposed by the open forest canopies are not tackled. In cases where a pixel is completely occupied by sunlit foliage and the shadow effects are small, such a bright-crown methodology would be successful. However, remote sensing pixels, even at sub-meter resolutions, generally contain both sunlit and shaded fractions. For retrieving leaf-level information from remote sensing measurements above conifer forests which are generally open and have distinct structural effects, new methodologies are yet to be developed. It is highly desirable to develop a methodology that is applicable to not only closed but also open canopies.

For retrieving leaf-level information from canopy-level measurements, the interactions of radiation with plant canopies need to be considered. Models based on radiosity (Borel et al., 1991; Goel et al., 1991), and ray tracing (Gastellu-Etchegorry et al., 1996; Myneni et al., 1990) can simulate the complexity of multiple scattering, but simplifications of the mathematical and canopy architectural descriptions are inevitable due to computational limitations (Gastellu-Etchegorry et al., 1996; Thompson & Goel, 1999). Geometrical–Optical (GO) models combine the advantages of simplicity, easy implementation, and capability of simulating the effects of canopy structure on the single and multiple scattering processes (Chen & Leblanc, 2001). GO models use geometrical shapes, such as cones for conifers and spheres or spheroids for deciduous trees, to simulate the angular and spatial distribution patterns of reflected solar radiance from forests (Chen & Leblanc, 1997; Li & Strahler, 1988; Li et al., 1995). When considering the complex canopy architectural conditions, Geometrical–Optical-Radiative Transfer (GO-RT) models seem to be a good solution to solve the multiple scattering issues, in which geometrical optics are used to describe the shadowing (the first order scattering) effects, and RT theories are adopted to estimate the second and higher order scattering effects. Chen and Leblanc (1997) developed the 4-Scale model using geometrical–optical theories. The applicable scale can range from leaves, whorls, crowns, and stands to the landscape. It is appropriate for analyzing surface scattering and scene compositions, and suitable for non-dense canopies for the study of structural change (Peddle et al., 2003), directional reflectance (Leblanc et al., 1999), forest structural parameters (Chen et al., 2005), and forest background information (Canisius & Chen, 2007).

The purpose of this paper is to develop a hyperspectral remote sensing algorithm for retrieving leaf chlorophyll content. The specific objectives are: (i) to investigate the feasibility of GO-RT models for retrieving leaf chlorophyll content of closed and, in particular, open

canopies; (ii) to develop a process-based methodology of retrieving leaf spectral reflectance from hyperspectral remote sensing imagery; (iii) to estimate leaf chlorophyll content through the combination of leaf and canopy-level model inversion; (iv) to compare this algorithm with spectral index methods on estimating leaf chlorophyll content; and (v) to retrieve leaf area index from hyperspectral remote sensing, and scale the leaf-level chlorophyll content estimates to the canopy-level. An example of a chlorophyll content image per unit ground surface area will be shown.

2. Data collection and processing

2.1. Study sites and leaf sampling

Ten black spruce (*Picea mariana* (Mill.), abbreviation SB) stands, within the area of 46° 49′ 13″ to 47° 12′ 9″ N, 81° 22′ 2″ to 81° 54′ 30″ W near Sudbury, Ontario, were selected as study sites (Fig. 1). The ten SB sites are of different ages, growth conditions, and crown closures. Of the ten sites, seven have very vigorous understorey species such as bog Labrador tea (*Ledum groenlandicum* Oeder), lichen (*Cladonia cristatella*), Feathery Bog-moss (*Sphagnum cuspidatum*), grass and bog rosemary (*Andromeda polifolia*). Three other sites are covered mainly by dense green moss. All the sites are easily accessible from roads and large enough (with a pure stand area of at least 20×50 m) for hyperspectral remote sensing image acquisitions. Near each site, at least two 2×2 m white ground targets were arranged as the ground control points to georeference the remote sensing images. Two 50 or 60-m-long parallel transects separated by 20 m were set up at each site in the east–west or southeast–northwest direction. Each transect was marked every 10 m using forest flags. In 2003 and 2004, field and laboratory measurements were carried out in four intensive field campaigns. Five medium trees from each site within a 20×20 m area were marked for shoot sampling and measurements of the average tree height and diameter at breast height (DBH). Shoots were sampled using a shotgun from the upper canopy, where needles are most exposed to sunlight. After sampling, shoots were immediately sealed in zip-lock plastic bags, and kept in a cooler with ice (the interior temperature of the cooler is 0 °C) for transport to a field laboratory for leaf spectral measurements and the subsequent needle biophysical and biochemical analysis.

Two aspen (*Populus tremuloides*) sites in the study region were also selected in 2003 to measure structural parameter leaf area index. Five trees of each site were sampled for measuring leaf optical spectra.

2.2. Leaf optical properties, biophysical and biochemical parameters

Within 12 h of the shoot sampling, five needles from each tree were measured for the reflectance and transmittance spectra. The new (year 2004) and old needles from the same tree were measured separately. Leaf reflectance and transmittance spectra were acquired based on the method of Harron and Miller (1995), which uses specially designed black anodized carriers to mount five needles in the spectral measurements. The average adaxial reflectance and transmittance were measured with a 1 nm spectral interval using a portable field spectroradiometer FieldSpec Pro FR (Analytical Spectral Devices, Inc. Boulder, USA) attached via a fiber optic cable to a Li-Cor 1800 integrating sphere (Li-Cor 1800-12S, Li-COR, Inc., Lincoln, Nebraska, USA). Leaf reflectance and transmittance spectra were weighted by the number of old and new needle samples (altogether 25 needles per site) to obtain the reflectance and transmittance of the site.

Fig. 1. Location of the ten black spruce (*Picea mariana* (Mill.)) study sites in Ontario, Canada, used in this research work.

Following the spectral measurements, needle thickness and width were measured using a digital calliper (Marathon Company, Canada). Needles were then stored in separate freezer bags and placed in a cooler with ice (the interior temperature of the cooler is 0 °C) for transport to the laboratory of the Ontario Forest Research Institute and stored at −23 °C. Leaf chlorophyll *a* and *b* contents were extracted and measured using the method described by Moorthy et al. (in press).

2.3. Needle-to-shoot area ratio

Of the ten black spruce sites, five sites with different canopy closures and ages were selected for the needle-to-shoot area ratio measurements. From each site, one medium tree was marked to collect branches from the top, middle, and bottom parts of the tree crowns. In addition, one site that is of medium canopy openness, growth condition, and tree height was sampled extensively to include a good variety of shoots. Three trees, one dominant, one co-dominant, and one suppressed tree were sampled from three heights of the crown: respectively top, middle, and bottom part. Samples were kept in portable electrical peltier coolers at a temperature slightly above 0 °C for laboratory analysis within one week after the sampling. For all the sampled branches, five shoots from each branch were analyzed. A digital camera (Toshiba PDR-4300) mounted on a firm copy stand (Regent Instruments Inc., Canada) was used to measure the shoot area projected on a light table (Kaiser Prolite 5000, Germany) at three camera incident angles: 0°, 45°, and 90° relative to the shoot main axis at 0° azimuth angle. The image analysis software WinSEEDLE (Regent Instruments Inc., Canada) was used to analyze the shoot projected area. Needle surface area in a shoot was determined using the volume displacement method described in Chen et al. (1997). Needle-to-shoot area ratio was derived based on the equation of Chen (1996), which includes the conversion of the projected shoot areas at multiple angles to the total shoot area.

2.4. Forest structural parameters

Three different optical instruments were used to measure leaf area index (LAI) and element clumping index (Ω_E) at each site following the recommendation of Chen et al. (1997). TRAC (Tracing Radiation and Architecture of Canopies, 3rd-Wave Engineering, Ottawa) instrument was operated under sunny conditions. Along two transects of 40–50 m at each site, TRAC measurements were tagged at each 10 m interval to mark the distance in the data stream. The effective LAI (L_e) was measured using the LAI-2000 (Plant Canopy Analyzer, LI-COR, Lincoln, NE) instrument and digital hemispherical photography (DHP) techniques at approximately the same time. These two instruments were operated around each 10 m flag on the two transects under overcast conditions or at either near dusk or dawn when the sun is below 75° from the zenith. For all the LAI-2000 measurements, a 90° view restrictor was used to block the direct light and to avoid the influence of the operator on the sensor. The operator always stood between the sensor and the sun. All hemispherical photographs were collected using a high resolution digital camera (4 Mega pixels) Nikon CoolPix 4500 with a Nikon FC-E8 fish-eye lens. The camera was mounted on a tripod to facilitate a horizontal camera setting, and the fish-eye lens was at nearly the same position and the same height of LAI-2000. The protocol proposed by Zhang et al. (2005) was adopted for the digital photo acquisition. Exposure setting was determined as a two stop overexposure relative to the automatic exposure of the sky outside of each stand.

2.5. Airborne hyperspectral remote sensing image

The reflectance imagery was acquired by the Compact Airborne Spectrographic Imager (CASI) over the ten black spruce sites in a *hyperspectral mode* at nadir on September 5, 2003. The CASI imagery provides 72 channels at a 7.5 nm spectral resolution covering the visible and near-infrared range from 408 nm to 947 nm and a 2 m spatial resolution. The images were radiometrically corrected to "at sensor" radiance by the Earth Observations Laboratory at York University. The atmospheric correction uses CAM5S and ground aerosol optical depth to obtain the ground-reflectance (O'Neill et al., 1997). The CASI imagery was then georeferenced using GPS data collected at the center of the sites and 2×2 m ground white targets that can be visually identified to accurately locate the sites. Flat field adjustments were applied to generate the final reflectance spectra. Average reflectance from pixels re-sampled to 20 m was used as input for analyses and modeling effort.

2.6. Forest background reflectance

The reflectance of dominant forest floor cover types were measured using the portable field spectroradiometer FieldSpec Pro FR (Analytical Spectral Devices, Inc. Boulder, USA) along the transects of each site under sunny conditions. Photos were taken around each 10 m forest flag using a digital camera (Toshiba PDR-4300). The camera lens was faced perpendicularly to the forest floor on homogeneous sunlit cover types and triggered by a remote control to avoid the operator's influence. The average areal fractions of major forest floor cover types were obtained by classifying the digital photos using the image processing software EARDAS. Based on the reflectance of the major cover types weighted by their corresponding areal fractions, forest background reflectance of the sites was derived.

The backgrounds of black spruce sites are composed of green moss and herbaceous understorey. The shrub-like understorey can cast shadows on the ground. During the measurements, the shadows of these targets are avoided. However, the site average reflectance should include these shadowing effects. The time, i.e., the solar zenith angle (SZA), for collecting forest background reflectance (SZA=50°) is different from that of the CASI image acquisition (from SZA=40° to SZA=44°). A bidirectional reflectance distribution function (BRDF) correction is performed to normalize the background reflectance of the ten black spruce sites to the sun-target-sensor geometry of the CASI data acquisition. BRDF correction coefficients are determined with a kernel-based BRDF model (Latifovic et al., 2003). The correction coefficients are determined by taking a ratio of the BRDF of the shrub type at nadir view and at the solar zenith angle during the measurements of the spectroradiometer (~50°) to the BRDF of the grass type at nadir and at the solar zenith angle during the CASI acquisition. The coefficients are calculated to be 0.86 and 0.74 for the visible and near-infrared region, which means that the visible and near-infrared reflectances are reduced by a factor of 0.86 and 0.74, respectively.

3. Methodology

Fig. 2 shows the flowchart of the leaf-level and canopy-level chlorophyll retrieval. The geometrical–optical model 4-Scale (Chen & Leblanc, 1997) and the leaf-level RT model PROSPECT (Jacquemoud & Baret, 1990) were combined to retrieve forest chlorophyll content. Forest canopy reflectance was simulated with the 4-Scale model. A look-up-table method, which is applicable to both open and closed canopies, was developed to invert the 4-Scale model for estimating leaf reflectance from canopy-level hyperspectral remote sensing imagery. With the estimated leaf reflectance, leaf chlorophyll content was estimated from the PROSPECT inversion model. Based on the retrieval of leaf chlorophyll content and a LAI map derived from the hyperspectral remote sensing imagery, forest chlorophyll content was mapped.

3.1. Estimation of canopy reflectance and forest scene components

To derive forest biochemical parameters accurately from hyperspectral remote sensing imagery, one approach is to estimate leaf reflectance spectrum from canopy-level hyperspectral data. To fulfill

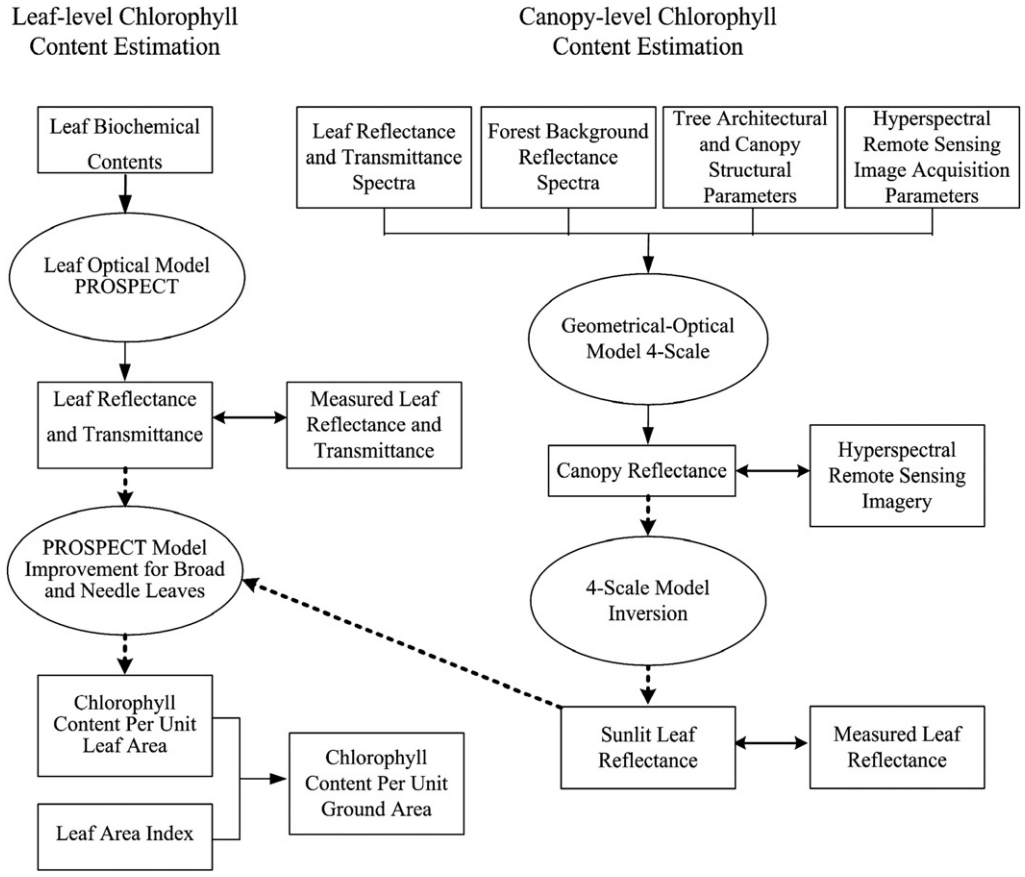

Fig. 2. Flowchart for leaf-level and canopy-level chlorophyll retrieval. In this chart, dashed lines represent inversion processes. The left right arrows represent the comparison for modeled and measured parameters.

this purpose, forest canopy reflectance needs to be estimated first. GO models estimate the anisotropic crown reflectance due to tree architecture and mutual shadowing among and within tree crowns by dividing the crown into two components: the sunlit and shaded foliage. Similarly, the sunlit and shaded backgrounds contribute to the overall reflectance of a pixel. Forest canopy reflectance is assumed to be a linear combination of these four components (Chen & Leblanc, 1997; Li & Strahler, 1988; Li et al., 1995):

$$R = R_T P_T + R_{ZT} P_{ZT} + R_G P_G + R_{ZG} P_{ZG} \quad (1)$$

where R is the canopy reflectance; R_T, R_{ZT}, R_G, and R_{ZG} are the reflectivities of sunlit tree crown, shaded tree crown, sunlit background, and shaded background, respectively; P_T, P_{ZT}, P_G and P_{ZG} are the probabilities of a sensor viewing sunlit and shaded tree crowns, sunlit and shaded background, respectively.

The GO model 4-Scale developed by Chen and Leblanc (1997) was used to estimate the canopy reflectance and the probabilities of viewing these four components. The model considers not only the spatial distribution of tree groups and the geometry of tree crowns, but also the structural effects of tree branches and scattering elements. Trees are simulated as non-random discrete objects with internal structures such as branches and shoots for coniferous types and leaves for deciduous types. A coniferous crown is simulated as a cone on top of a cylinder, and a deciduous crown as a spheroid with variable vertical and horizontal dimensions. Trees spatially follow a Neyman distribution to simulate patchiness of a forest stand. Each crown is taken as a complex medium, in which the mutual shadowing occurs between shoots of coniferous types and leaves of deciduous types, so that even on the sunlit side of the crown, the shaded foliage could be observed by the sensor. A multiple scattering scheme, which is based on view factors among the four components in canopies, is incorporated in the model to simulate the angular variation in the multiple scattering processes (Chen & Leblanc, 2001).

The 4-Scale model was run to estimate canopy reflectance with inputs of leaf optical properties, forest background reflectance spectra, and parameters of tree architecture, canopy structure, and image view geometry. For black spruce species, field and laboratory measurements provide the required canopy structural parameters, leaf and forest background optical properties. The viewing geometry parameters were derived from the CASI image acquisition campaigns. For deciduous species, as only leaf optical spectra and image viewing geometry parameters were available. Chen and Leblanc (1997) defined a set of general tree architectural parameters for coniferous and deciduous canopies separately. Table 1 lists the forest parameters input to the 4-Scale model for black spruce and deciduous species.

3.2. GO model inversion for estimating leaf reflectance

The objective of model inversion is to estimate the contribution of an individual sunlit leaf to the measured canopy-level reflectance R

Table 1
Input parameters to the 4-Scale model to generate LUTs for black spruce and deciduous species

4-Scale model parameters	Black spruce	Deciduous
Number of trees per ha	3500	2000
Tree shape	Cone+cylinder	Spheroid
Stick height (m)	5	10
Crown height (m)	10	10
Radius of crown (m)	0.5	2

across the spectrum. The canopy reflectance R derived from remote sensing images is the combination of the contributions from all forest scene components. Each pixel represents an assemblage of green and non-green plant portions including leaves, twigs, bark, and forest background. The reflectivity of the sunlit foliage simulated by the model (R_T) is accordingly the reflectivity of an assemblage of sunlit leaves. R_T is different from the reflectivity of an individual leaf due to leaf angle distribution and multiple scattering effects inside the canopy. In the 4-Scale model, a phase function is used to estimate the distribution of scattered radiation from a foliage element (shoot for conifer, leaf for broadleaf forest) with view angle. Multiple scattering effects are strong in forests, which can enhance the leaf absorption features up to a factor of 2 (Baret et al., 1994). To convert the reflectivity of the sunlit foliage (R_T) to the reflectivity of an individual leaf R_L, a multiple scattering factor M_0 is introduced:

$$R_T = R_L \times M_0 \tag{2}$$

This factor also accounts for the effect of the leaf phase function determining the first order scattering at various view directions relative to the illumination direction.

The shaded foliage and background components result from diffuse radiation from the sky and multiple scattering. The reflectivity of the shaded foliage and shaded background can be expressed as follows:

$$R_{ZT} = R_T \times \frac{S_{Sdif}}{S_g} \times M_0 \tag{3}$$

$$R_{ZG} = R_G \times \frac{S_{SGdif}}{S_g} \times M_0 \tag{4}$$

where S_g is the total incoming solar irradiance. S_{Sdif} is the diffuse irradiance on the shaded leaves, S_{SGdif} is the diffuse irradiance on the shaded background. $\frac{S_{Sdif}}{S_g}$ and $\frac{S_{SGdif}}{S_g}$ are respectively the fractions of diffuse irradiance in the total incoming solar irradiance above and below the stand. Compared with the sunlit reflectivities, the shaded reflectivities are small. The contribution of the shaded leaves and shaded background can be incorporated in the first term of Eq. (1). Therefore, a multiple scattering factor M, which includes the contributions of the two shaded components, was introduced to convert R_T to R_L. The Eq. (1) becomes:

$$M = \frac{R - R_G \times P_G}{R_L \times P_T} \tag{5}$$

Given that canopy reflectance R can be remotely measured and forest background reflectivity R_G is known, the probabilities of observing the sunlit foliage (P_T) and background (P_G) components and the spectral multiple scattering factor (M) need to be estimated to invert the individual leaf reflectivity R_L. Different methodologies can be carried out for the estimation of biophysical canopy parameters by numerical model inversion. The look-up table (LUT) is conceptually the simplest method (Pragnère et al., 1999). Two LUTs were developed using the 4-Scale model to take into account different canopy structural configurations and viewing geometry. At given SZA, view zenith angle (VZA), and azimuthal angle between sun and view (PHI), variations of R, P_T, and P_G depend on stem density, LAI, tree height, and radius of tree crown. The sensitivity of R, P_T, and P_G to these model input parameters was investigated to develop the LUTs. For simplicity, two LUTs were developed as functions of viewing geometry (VZA, SZA, and PHI) and one dominant contributor for both black spruce and deciduous species. One LUT provides the probabilities of viewing the sunlit foliage P_T and background P_G components, and the other LUT provides the spectral multiple scattering factors MS to convert the average reflectivity of sunlit leaves to the reflectivity of an individual sunlit leaf.

Combining the two LUTs, forest background reflectance measurements, and canopy reflectance derived from CASI, the sunlit leaf reflectivity R_L can be derived:

$$R_L = \frac{R_{CASI} - R_G \times P_G}{P_T \times M} \tag{6}$$

where R_{CASI} is the reflectance of the site from the re-sampled 20 m CASI imagery.

3.3. Leaf-level chlorophyll content retrieval

The leaf model PROSPECT simulates leaf reflectance and transmittance based on Allen's multilayer plate model (Allen et al., 1969). Leaf biochemical contents can be estimated from measured leaf spectra through numerical iteration to minimize the difference between measured and estimated leaf spectra. The model is validated widely with several broadleaf species. It has been improved to simulate seasonal and canopy-height related variation in broadleaf chlorophyll content (Zhang et al., 2007) and modified for applications to conifer needles by introducing needle thickness and width to take into account the effects of needle shape on radiation scattering (Zhang et al., 2008).

PROSPECT model requires leaf reflectance and transmittance spectra as inputs to estimate leaf chlorophyll content. In this study, the original and modified PROSPECT models were applied separately to deciduous, grass, and coniferous species for estimating broad leaf and needle chlorophyll contents. Based on the inverted needle/broad leaf reflectance from Eq. (6), and spectral ratio of the corresponding measured needle/broad leaf reflectance to transmittance spectra, needle/broad leaf transmittance spectra can be derived. For needles, as the measured transmittance is low in the red region from 650 nm to 690 nm, the ratio of the spectrally averaged reflectance to transmittance was applied in the derivation of needle transmittance in this low signal region. With all the measured needle/broad leaf spectra available, it is found that using the average spectral ratio of measured leaf reflectance to transmittance to derive leaf transmittance incurs bias estimation of chlorophyll content by −5.2% to 8.4%. The Li-Cor 1800 lamp emits UV-violet light at very low intensities, which results in noisy spectral signals in the needle spectra in the 400–500 nm region, only wavelengths beyond 450 nm was included in the inversion of needle chlorophyll content. As no leaf spectra were measured for the grass type, the reflectance of grass type obtained from the CASI imageries was taken as a surrogate of the reflectance of grass leaves. It is found that the grass shows similar spectra to that of sugar maple leaves (Mohammed et al., 2000). The spectral ratio of sugar maple leaves based on measurements by Zhang et al. (2007) was applied to grass type to derive transmittance spectra of grass.

The root mean square error (RMSE) in estimates was computed to estimate the deviation between the estimated and measured chlorophyll content:

$$\mathrm{RMSE} = \sqrt{\frac{1}{m}\sum_{i=1}^{m}\left(\hat{y}_i - y_i\right)^2} \tag{7}$$

where $\hat{y}_i$ is the chlorophyll content estimate based on model inversion or an empirical spectral index, and y_i is the corresponding measured chlorophyll content; m is the number of leaf samples. The estimates were then subject to an intensive cross-validation procedure using a jackknife re-sample technique (Miller, 1964, 1968). RMSE was calculated on the reduced sample by leaving out one sample at a time from the whole sample set. The procedure was repeated until all samples are evaluated. As a comparison, two spectral indices (Sims & Gamon, 2002), the modified Simple Ratio index (mSR): $(R_{728}-R_{434})/(R_{720}-R_{434})$, and the modified Normalized Difference index (mND): $(R_{728}-R_{720})/(R_{728}+R_{720}--2*R_{434})$, were investigated for the estimation of needle chlorophyll content.

Two chlorophyll spectral indices, TCARI/OSVAI developed by Haboudane et al. (2002) and MTCI by Dash and Curran (2004), were adopted to evaluate their correlation to chlorophyll content at leaf and canopy scales. These two spectral indices were developed based on modelled spectra, field spectra, and airborne/spaceborne remote sensing data, so may be viewed as semi-empirical indices sensitive to chlorophyll content. TCARI/OSVAI minimizes the effects of varying LAI and soil background using narrow-band remote sensing data and has been reported to be suitable for crop, as well as open and structured canopies (Haboudane, 2002; Zarco-Tejada et al., 2004b, 2005). MTCI relates a measure of the red-edge position with canopy chlorophyll content (Dash & Curran, 2004).

3.4. LAI retrieval and forest chlorophyll content mapping

LAI is an important forest structural variable to scale up leaf-level biochemical parameters to a canopy scale. Satellite digital imagery has demonstrated utility for LAI retrieval (Badhwar et al., 1986; Chen & Cihlar, 1996; Hall et al., 1995; Nemani et al., 1993; Peterson et al., 1987). Airborne remote sensing technology has the advantage over satellite data in terms of reducing uncertainties and errors in the process of image registration, atmospheric correction, and matching of image and ground measurements. Airborne hyperspectral CASI data with high spatial resolution can reproduce the heterogeneity of ground surface, and is effective to derive forest biophysical parameters (Chen et al., 1999). Vegetation indices have been found to correlate with ground-based LAI measurements. The Normalized Difference Vegetation Index (NDVI), Simple Ratio (SR), and Reduced Simple Ratio (RSR) are commonly used indices for retrieving LAI. Chen and Cihlar (1996) found SR is more linearly related to LAI than NDVI in boreal forest. This study explored the SR algorithm, calculated as:

$$\mathrm{SR} = \frac{\rho_{\mathrm{NIR}}}{\rho_{\mathrm{red}}} \tag{8}$$

As the effects of shadows in open canopies are large, recommendations of Chen et al. (1999) were followed to minimize the effects of forest background on the LAI retrieval. Reflectance of the fine resolution (2 m) images was spectrally averaged to calculate SR first, and the spatially averaged SR of 20×20 m pixel was then taken as SR of the site to explore the correlation with ground-measured LAI. As LAI of deciduous species and grass were not measured, the SR-LAI correlations developed by Chen et al. (2002) were adopted for retrieving LAI of these two species.

Forest chlorophyll content was mapped through the following procedure: (i) to generate a fine resolution (2×2 m) land cover image through image classification. The vegetated area in CASI imagery was stratified into three categories: coniferous, deciduous, and grass cover types; (ii) to produce a coarse resolution (20×20 m) LAI image based on the land cover image and results of the LAI retrieval; and (iii) to map vegetation chlorophyll content (per unit ground area) using the LAI image and retrieved leaf chlorophyll content (per unit leaf area) described in Section 3.3.

4. Results

4.1. Canopy reflectance estimates

The ten sites have a good variety of tree heights, tree diameters, leaf chlorophyll content, foliage coverage, and clumping (Table 2). The viewing geometry of the CASI images over the sites ranges from SZA of 40° to 44° (Table 2).

Fig. 3 shows an example of the measured needle reflectance and transmittance spectra, and forest background reflectance spectra after BRDF correction of one black spruce site as inputs to the 4-Scale model. One site (SB8) with medium foliage coverage and clumping was selected for the LUT development. Fig. 4 shows the comparisons of estimated canopy reflectance and CASI measurements for the other nine sites. The model captures the feature of canopy reflectance from the visible to the near-infrared ranges, with slight discrepancies (0.24% to 3.28%) between the estimated and measured reflectance in the blue region, and in the green and red region (0.01% to 1.60%). Discrepancies are much larger in the near-infrared region (0.00% to 4.44%), where CASI reflectance from bands 69 to 72 is inconsistent as the sensitivity of the sensor is low at longer wavelengths and the atmospheric water absorption was not corrected. In the chlorophyll absorption sensitive region (the red and red-edge region), discrepancy between the estimated canopy reflectance and CASI measurements is 0.06%–1.07% in the average red reflectance and 0.36%–1.63% in the average red-edge reflectance (Table 3). Discrepancy of the chlorophyll sensitive red-edge index (R_{750}/R_{710}) is in a range of 0.021 to 0.043 (Table 3).

4.2. LUTs and leaf reflectance retrieval

The 4-Scale model was run to investigate the sensitivity of canopy reflectance, P_T, and P_G to input parameters. Table 4 shows the variations of P_T, P_G, and red-edge index (R_{750}/R_{710}) under a range of stem density, LAI, tree height, and radius of tree crown for black spruce species. At a given viewing geometry, LAI is the dominant, and stem density is the secondary factor contributing to P_T, P_G, and canopy reflectance. Increase of LAI from 1 to 5 results in an increase of P_T by 5.5%–32.3% and R_{750}/R_{710} by 1.3%–4.4%, and a decrease of P_G by 15.5%–28.3%. When the stem density is changed from 2000 to 4500 trees per ha, P_T increases by 7.1%–9.8%, P_G decreases by 7.6%–14.3%, and the optical index R_{750}/R_{710} increases by 0.4%–1.8%. Compared to LAI, the effects of stand density on the canopy reflectance is small. Doubling LAI results in an increase of the red-edge index R_{750}/R_{710} by 4.7%–7.5%, while doubling of stand density causes an increase of R_{750}/R_{710} by 4.1%–5.3%. However, LAI and stand density are often correlated in reality. For simplicity, this study developed LUTs as a function of LAI, VZA, SZA, and PHI for both the black spruce and deciduous species. For each species, two LUTs were developed to provide the probabilities of viewing sunlit foliage and sunlit background, and the spectral multiple scattering factors, with LAI ranging from 0.1 to 6 in steps of 0.1, VZA from 0° to 45° in steps of 15°, and SZA from 0° to 70° in steps of 10°. Tables 5 and 6 are the two sample LUTs for the black spruce

Table 2
Black spruce (SB) site parameters: tree diameter at breast height (DBH), clumping index (Ω_E), leaf area index (LAI), average total chlorophyll content (Chlorophyll$_{a+b}$), needle-to-shoot area ratio (γ_e), view zenith angle (VZA), solar zenith angle (SZA), and azimuthal angle between sun and view (PHI)

Site	Longitude (°W)	Latitude (°N)	Tree height (m)	DBH (cm)	Ω_E	LAI	Chlorophyll$_{a+b}$ (μg/cm^2)	γ_e	VZA (°)	SZA (°)	PHI (°)
SB1	81.742	47.164	13.89±1.63	15.44±1.38	0.79	3.30	32.68±5.62		0	40.38	0
SB2	81.908	47.202	15.72±1.12	19.60±1.75	0.81	3.97	25.01±2.26		0	40.50	0
SB3	81.368	46.821	14.08±0.73	16.38±1.97	0.88	2.36	37.30±4.38	1.5276	0	43.66	0
SB4	81.375	46.820	17.78±2.37	18.28±3.39	0.84	3.21	33.64±11.06	1.4537	0	44.20	0
SB5	81.420	46.907	12.58±2.31	12.14±1.88	0.80	3.09	31.18±6.80		0	40.28	0
SB6	81.743	47.164	17.10±1.47	14.78±2.77	0.77	3.78	37.61±4.38	1.3564	0	40.38	0
SB7	81.746	47.163	4.90±2.02	5.58±2.89	0.85	1.14	30.76±3.39		0	40.38	0
SB8	81.727	47.162	6.56±3.03	6.58±2.73	0.84	2.88	28.34±5.21	1.4876	0	40.38	0
SB9	81.867	47.199	11.20±0.83	10.22±1.15	0.84	3.83	24.96±10.54	1.4783	0	40.44	0
SB10	81.908	47.203	13.28±2.46	15.08±4.01	0.81	5.37	34.99±7.65		0	40.50	0

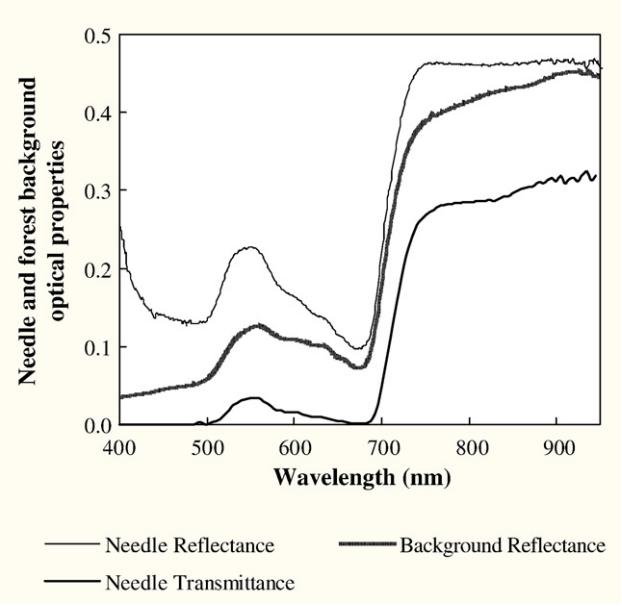

Fig. 3. Needle reflectance and transmittance spectra, and forest background reflectance of one black spruce site used as inputs to the 4-Scale model.

species. The contributions of the sunlit foliage and the sunlit background vary with the view angle. At the nadir view, P_T is the minimum while P_G is the maximum. When VZA varies from 30° to 45°, P_T increases while P_G decreases. At a given VZA and at nadir for the CASI imagery in this study, the contributions of the sunlit foliage and background to the total canopy reflectance can be seen from Fig. 5a and b. The probabilities of viewing sunlit foliage (P_T) and background (P_G) vary with LAI and SZA. P_T increases as the foliage coverage (LAI) increases, while P_G decreases as LAI increases. When LAI increases from 1 to 2, the change of P_T and P_G are dramatic, with an increase of P_T ranging from 29.1% to 32.5% and a decrease of P_G ranging from 15.5% to 53.2%. When LAI is above 2, P_T increases and P_G decreases gradually. Clumping of needles affects both the magnitudes of these probabilities and rates of their changes with LAI. Both P_T and P_G decrease as the shaded components increase with SZA.

The effect of LAI to the multiple scattering factor M is partially shown in Table 6. M increases with the increase of LAI. In the visible region, the values of M are smaller than 1, while in the near-infrared region, M are greater than 1. When the observed sunlit foliage component is estimated, the mutual shadowing effects of leaves on the sunlit side of tree crown is already considered in 4-Scale, which treats a crown surface as a complex surface rather than an imaginary smooth surface. The variation of reflected radiance with the leaf angle relative to the sun's direction is quantified using a phase function in the 4-Scale model. Because of the variable orientations of leaves relative to the sun's direction, the reflectance of combined sunlit leaves is lower than that of a leaf perpendicular to the sun (in leaf spectral measurements, incident light is perpendicular to the leaf surface). To convert a reflectance spectra of an aggregated sunlit foliage to that of a fully sunlit leaf, the spectral multiple scattering factor is therefore smaller than 1 in the visible region. In the near-

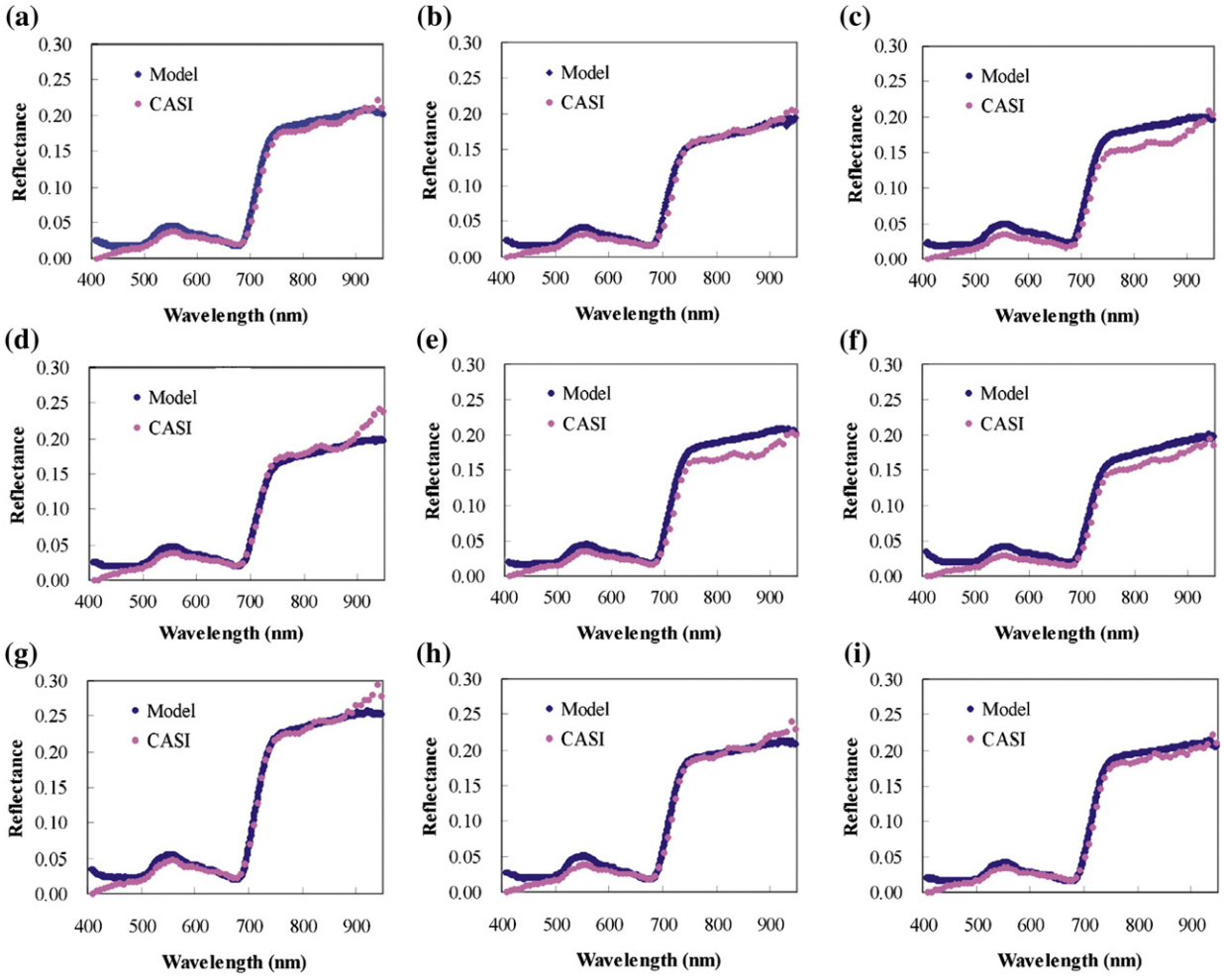

Fig. 4. Comparison of the canopy reflectance from the 4-Scale model and from the CASI images for the nine black spruce sites.

Table 3
The discrepancy of the red-edge index (R_{750}/R_{710}), average red reflectance (R_{red}), and average red-edge reflectance ($R_{red\text{-}edge}$) between the 4-Scale model estimation and the CASI measurements for different sites

	SB1	SB2	SB3	SB4	SB5	SB6	SB7	SB9	SB10
R_{750}/R_{710}	0.029	0.035	0.021	0.022	0.028	0.038	0.021	0.030	0.043
R_{red}	0.06%	0.24%	0.73%	0.12%	0.35%	0.66%	0.08%	0.12%	1.07%
$R_{red\text{-}edge}$	0.36%	0.43%	0.73%	1.63%	0.49%	0.32%	1.54%	0.90%	0.61%

infrared region, however, multiple scattering is strong due to large leaf reflectance and transmittance. This strong multiple scattering could more than compensate the phase function effect, making the multiple scattering factor greater than 1.

Sunlit leaf reflectance of both the black spruce and the deciduous species were retrieved. Table 7 shows the comparison of the retrieved and measured leaf reflectance for the black spruce species. The retrieved leaf reflectance is in reasonable agreement with the laboratory measured leaf reflectance. The discrepancy between estimated and measured leaf reflectance is 0.02%–3.63% in the average red reflectance and 0.24%–7.88% in the average red-edge reflectance. The discrepancy of the chlorophyll sensitive red-edge index (R_{750}/R_{710}) is in a range of 0.001 to 0.024. Across the spectrum, the estimated and measured leaf reflectance demonstrate a good correlation (R^2=0.89 to R^2=0.97), with poor correlation found in the blue region (400–500 nm) and beyond band 69 (916 nm).

It is found that the retrieval of leaf reflectance is sensitive to the canopy reflectance. The discrepancy between the estimated canopy reflectance and CASI measurements, for example, from 400 nm to 450 nm (Fig. 4), causes a large discrepancy between the inverted and measured leaf reflectance. In the near-infrared region, small variation in the CASI reflectance results in large discrepancies (0.01%–11.80% from 700 to 908 nm) between the measured and inverted leaf reflectance. From bands 69 to 72, the discrepancy is large due to the inconsistency in the CASI reflectance. In the red region (600–700 nm) where the leaf has strong absorption, the model generates good estimates. The discrepancy between the inverted and measured leaf reflectance is in a range of 0.04% to 4.45%.

Table 4
Sensitivity of the probability of viewing sunlit foliage (P_T) and sunlit background (P_G), and chlorophyll sensitive index R_{750}/R_{710} to stem density, LAI, tree height, and radius of tree crowns

Parameter and value		P_T	P_G	R_{750}/R_{710}
LAI	1	0.095	0.611	1.778
	2	0.126	0.438	1.861
	3	0.141	0.340	1.922
	4	0.150	0.277	1.954
	5	0.158	0.234	1.981
Stem density (number of trees per ha)	2000	0.111	0.390	1.882
	2500	0.123	0.341	1.917
	3000	0.135	0.306	1.944
	3500	0.148	0.278	1.954
	4000	0.161	0.256	1.963
	4500	0.174	0.238	1.955
Tree height (m)	5	0.146	0.300	1.860
	6	0.148	0.285	1.876
	7	0.149	0.272	1.893
	8	0.150	0.262	1.910
	9	0.151	0.254	1.919
	10	0.152	0.247	1.945
	11	0.153	0.241	1.945
	12	0.154	0.236	1.955
	13	0.154	0.232	1.955
	14	0.155	0.227	1.964
	15	0.155	0.224	1.973
Radius of tree (m)	0.4	0.130	0.279	1.898
	0.5	0.147	0.238	1.898
	0.6	0.156	0.205	1.876
	0.7	0.159	0.179	1.883
	0.8	0.155	0.158	1.878
	0.9	0.148	0.142	1.894
	1.0	0.138	0.129	1.900

Table 5
Sample look-up table for black spruce species for the probabilities of viewing sunlit foliage (P_T) and sunlit background (P_G) by the sensor as functions of leaf area index (LAI), view zenith angle (VZA), solar zenith angle (SZA), and azimuthal angle between the sun and view (PHI)

LAI	P_T	P_G	VZA	SZA	PHI
1.0	0.1245	0.6486	0	30	0
1.1	0.1303	0.6275	0	30	0
1.2	0.1354	0.6080	0	30	0
1.3	0.1401	0.5898	0	30	0
1.4	0.1443	0.5727	0	30	0
1.5	0.1481	0.5568	0	30	0
1.6	0.1188	0.4862	0	40	0
1.7	0.1213	0.4708	0	40	0
1.8	0.1236	0.4563	0	40	0
1.9	0.1257	0.4426	0	40	0
2.0	0.1276	0.4297	0	40	0
2.1	0.2920	0.3714	30	40	0
2.2	0.3000	0.3581	30	40	0
2.3	0.3077	0.3455	30	40	0
2.4	0.3151	0.3336	30	40	0
2.5	0.3223	0.3224	30	40	0
2.6	0.3950	0.3174	45	40	0
2.7	0.4025	0.3074	45	40	0
2.8	0.4098	0.2980	45	40	0
2.9	0.4169	0.2891	45	40	0
3.0	0.4238	0.2806	45	40	0

4.3. Chlorophyll content retrieval and mapping

Fig. 6 shows the results of needle chlorophyll content retrieval for the black spruce sites using the modeling approach. Compared to the ground-measured average needle chlorophyll$_{a+b}$ content, the estimation yields an accuracy of R^2=0.47 and RMSE=4.34 μg/cm^2 for the nine sites with chlorophyll$_{a+b}$ content ranging from 24.9 μg/cm^2 to 37.6 μg/cm^2. The jackknifed RMSE is 5.69 μg/cm^2. The R^2 of chlorophyll

Table 6
Sample look-up table for black spruce species for the spectral multiple scattering factor (M) as functions of leaf area index (LAI), view zenith angle (VZA), solar zenith angle (SZA), and azimuthal angle between the sun and view (PHI)

Wavelength (nm)	LAI=2	LAI=3	LAI=4	LAI=5
400	0.6866	0.7429	0.7656	0.7818
401	0.6705	0.7318	0.7570	0.7751
402	0.6633	0.7244	0.7497	0.7678
403	0.6816	0.7137	0.7418	0.7619
404	0.6733	0.7106	0.7418	0.7642
405	0.6643	0.7071	0.7418	0.7668
406	0.6387	0.7213	0.7245	0.7517
407	0.6257	0.7161	0.7216	0.7517
408	0.6512	0.7080	0.7161	0.7491
409	0.6261	0.6888	0.6995	0.7352
410	0.6337	0.6980	0.7093	0.7457
411	0.6327	0.6979	0.7096	0.7111
412	0.6277	0.6933	0.7053	0.7421
413	0.6017	0.6739	0.6888	0.7286
414	0.6050	0.6786	0.6940	0.7344
750	1.0468	1.3180	1.4242	1.4727
751	1.0380	1.3262	1.4182	1.4673
752	1.0485	1.3219	1.4294	1.4785
753	1.0422	1.3327	1.4258	1.4755
754	1.0530	1.3282	1.4366	1.4862
755	1.0468	1.3390	1.4329	1.4831
756	1.0575	1.3342	1.4289	1.4797
757	1.0524	1.3308	1.4408	1.4914
758	1.0467	1.3418	1.4373	1.4884
759	1.0563	1.3360	1.4468	1.4978
760	1.0491	1.3468	1.4437	1.4955

Here VZA=0°, SZA=40°, and PHI=0°.

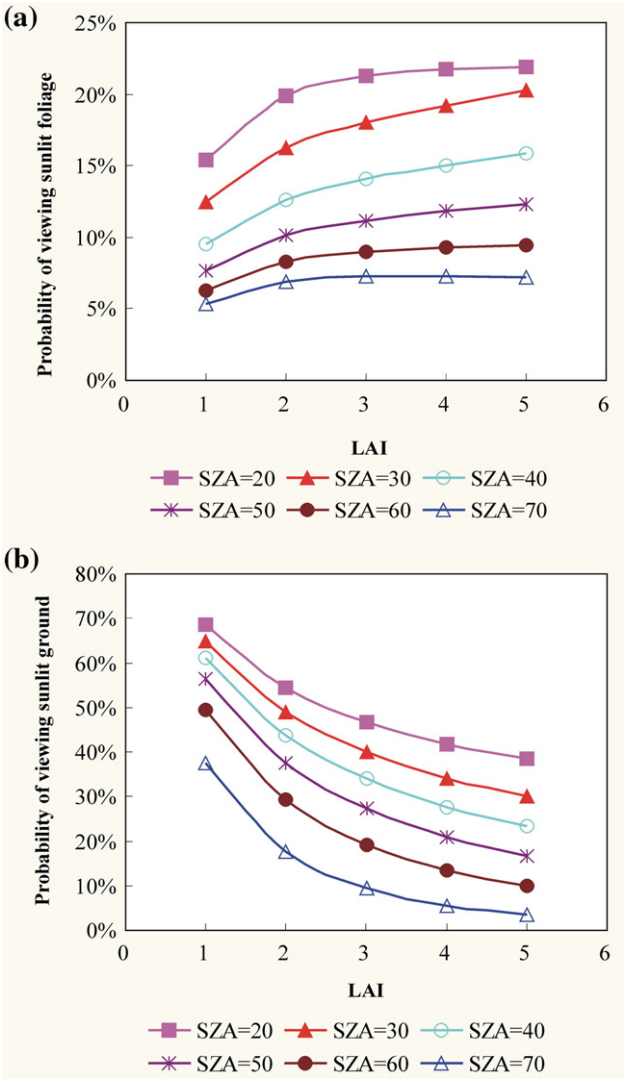

Fig. 5. Probabilities of forest scene components estimated by the 4-Scale model. (a) Probabilities of viewing sunlit foliage at nadir view with change of leaf area index (LAI) and solar zenith angle (SZA). (b) Probabilities of viewing sunlit background at nadir view with change of leaf area index (LAI) and solar zenith angle (SZA).

estimation for black spruce needles using mND and mSR are 0.17 and 0.21, respectively. The relationship between the chlorophyll$_{a+b}$ estimates from the model and ground-based measurements has a slope close to 1 (0.803) and a small interception (4.27), indicating that the modeling approach produces systematically fair estimation.

The two chlorophyll indices MTCI and TCARI/OSAVI show the expected variation with leaf and canopy chlorophyll$_{a+b}$ content over the nine sites (Table 8). TCARI/OSAVI correlates better with leaf chlorophyll$_{a+b}$. But with its relative insensitivity to LAI variations, it shows only poor relationship with canopy chlorophyll$_{a+b}$ content. In this study, the forest background has a green and variable vegetation signature instead of bare soil. The relationship of TCARI/OSAVI to canopy chlorophyll$_{a+b}$ content is not as tight as those shown for crop canopies or open canopies (Haboudane et al., 2002; Zarco-Tejada et al., 2004b, 2005). MTCI shows a good relationship with canopy chlorophyll$_{a+b}$ content, as it is based on a measure of the red-edge position which is influenced by both leaf chlorophyll content and LAI. However, it shows no measurable correlation with leaf chlorophyll$_{a+b}$ content because of the confounding effect of LAI variations. For both indices when applied to open boreal canopies, a strong influence of the vegetated understorey remains as a perturbing parameter.

Table 7
The discrepancy of the red-edge index (R_{750}/R_{710}), the average red reflectance (R_{red}), and the red-edge reflectance ($R_{red\text{-}edge}$) between the 4-Scale model inversion and the measured leaf reflectance for different sites

	SB1	SB2	SB3	SB4	SB5	SB6	SB7	SB9	SB10
R_{750}/R_{710}	0.011	0.024	0.003	0.001	0.022	0.022	0.001	0.009	0.018
R_{red}	0.02%	1.69%	2.31%	0.08%	3.63%	2.46%	0.25%	1.50%	0.13%
$R_{red\text{-}edge}$	0.24%	1.57%	3.78%	3.43%	7.88%	2.91%	0.59%	2.91%	1.31%

With the mean background SR value from the field measurements, and the spatially and spectrally coarsened SR from CASI imagery versus LAI measurements of the nine black spruce sites, the SR–LAI relationship is developed (Fig. 7). SR can explain 88% of the LAI variation. When the canopy is open, the effect of forest background is large. The background is often visually greener than the forest canopy. SR is high even under low LAI, which may be due to the abundant understorey and moss ground cover of the sites. The original 2 m resolution CASI imagery was classified into water body, land, grass, coniferous and deciduous forest species. The 20 m resolution land cover map was produced based on the dominant cover types in the 2 m CASI land cover imagery. Combined with SR-LAI correlations, a final CASI LAI coverage was generated (Plate I). In this image, the proportions of coniferous species, deciduous species, and grass are respectively 53.2%, 16.1%, and 21.4%. LAI of the vegetated regions ranges from 0.18 to 5.40. The highest LAI values are found from the deciduous forest species.

Leaf chlorophyll$_{a+b}$ contents for the three cover types were estimated from the re-sampled 20 m resolution CASI image (Plate II). The predicted chlorophyll$_{a+b}$ content ranges from 24.1 μg/cm^2 to 35.9 μg/cm^2 for the black spruce species, 27.2 μg/cm^2 to 43.4 μg/cm^2 for the deciduous species, and 20.1 μg/cm^2 to 23.4 μg/cm^2 for the grass species. Combined with LAI, this output was used to estimate chlorophyll$_{a+b}$ content per unit ground surface area (Plate III). Chlorophyll$_{a+b}$ content per unit ground surface area ranged from 30 mg/m^2 to 2170 mg/m^2 for vegetated pixels.

5. Discussion

Changes in leaf chlorophyll content result in variation of leaf reflectance and transmittance spectra in the visible region, which contribute to the canopy reflectance. Canopy reflectance is also strongly affected by other factors such as canopy architecture, chlorophyll distribution in the canopy, sun/view angle, and forest background. These

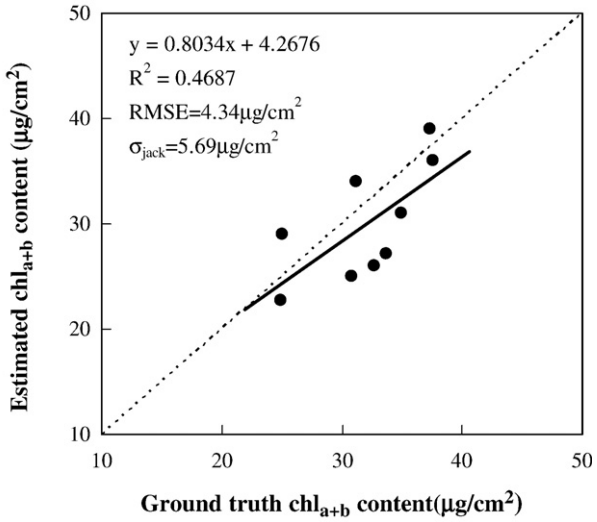

Fig. 6. Relationship between the needle chlorophyll content from the measurements and from the modified PROSPECT model (The dotted line is the 1:1 line.). The jackknifed residual is shown in the figure.

Table 8
Performance of TCARI/OSAVI and MTCI index for estimating chlorophyll content at leaf and canopy scales (y denotes leaf/canopy chlorophyll content, x denotes index)

Index	Correlation to leaf chlorophyll content	Correlation to canopy chlorophyll content
TCARI/OSAVI	$y=-12.41\mathrm{Ln}(x)+8.5886$, $R^2=0.4025$	$y=-81.998\mathrm{Ln}(x)-48.634$, $R^2=0.1915$
MTCI	$y=53.265x^2-204.51x+226.05$, $R^2=0.2005$	$y=151.29(x)-184.35$, $R^2=0.6456$

factors mask and confound changes in canopy reflectance caused by leaf chlorophyll content, which makes chlorophyll retrieval at the canopy-level complicated and challenging. This study handles this complex issue using process-based models, which are especially necessary for the open forest canopies. Compared with empirical correlations and radiation transfer models that assume the canopy is spatially homogeneous, the GO model 4-Scale takes into account the complex canopy structural effects, and the leaf model considers light interactions with the foliar medium and the complexity of leaf internal structure. This study demonstrates that the model can mimic the reality of the open and clumped nature of boreal forests. The LUT method for the 4-Scale model inversion is applicable for both deciduous and coniferous species. The LUTs consider detailed canopy information and viewing geometry, and separate the canopy structural effects from leaf optical properties. Combination of process-based leaf and canopy-level models is feasible for retrieving chlorophyll content of needle and broad leaf species from hyperspectral remote sensing images.

Accurate measurements of leaf optical properties, forest background reflectance, and forest structural parameter LAI are the key to the success of leaf reflectance retrieval, and thus the leaf chlorophyll retrieval from remote sensing imagery. As seen from the discrepancy between the estimated canopy reflectance and the CASI measured reflectance, the noisy signals in needle reflectance spectra in the blue region (400–450 nm) cause opposite variations. The discrepancy can cause bias estimates of the spectral multiple scattering factor. As the multiple scattering factor incorporates effects of leaf angle distribution, and the contributions from the shaded foliage and background, the bias is enlarged in the retrieval of sunlit leaf reflectance from remote sensing imagery.

LAI is the dominant factor that determines the amplitude of canopy reflectance, fractions of viewing forest scene components, spectral multiple scattering, and thus the retrieval of leaf reflectance from remote sensing imagery. As LAI measurements only include tree canopy, LAI of the sites is actually the overstorey LAI. Open boreal forests have clumped and open overstorey, and dense, vigorous, and variable understorey which contribute to the above-canopy reflectance measured by the sensor. For the black spruce species in this study, the forest background is mainly covered by vigorous green moss and herbaceous understorey. The relationship of ground-measured LAI and SR derived from remote sensing imagery may have some bias. In addition, due to the heterogeneity of the forest background, the retrieved overstorey LAI distribution from SR may not fully represent the variations in reality.

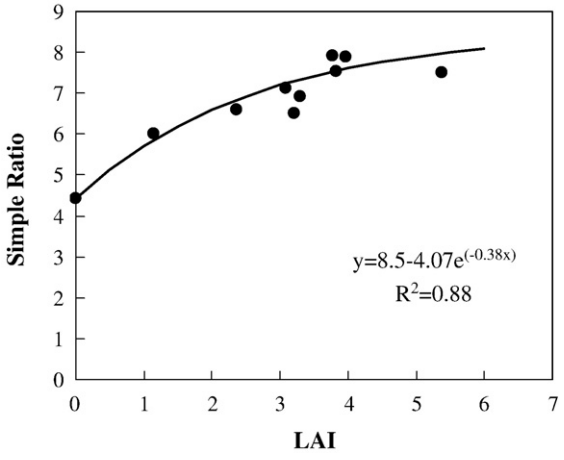

Fig. 7. Correlation between vegetation index SR derived from the CASI images and ground-based LAI measurements.

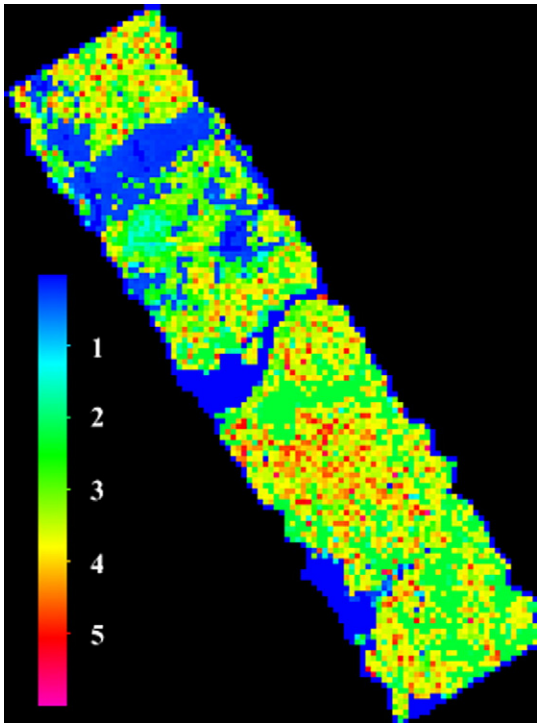

Plate I. CASI LAI image over one black spruce site. The image is derived based on the SR-LAI relationship and land cover image. The spatial resolution of the image is 20×20 m.

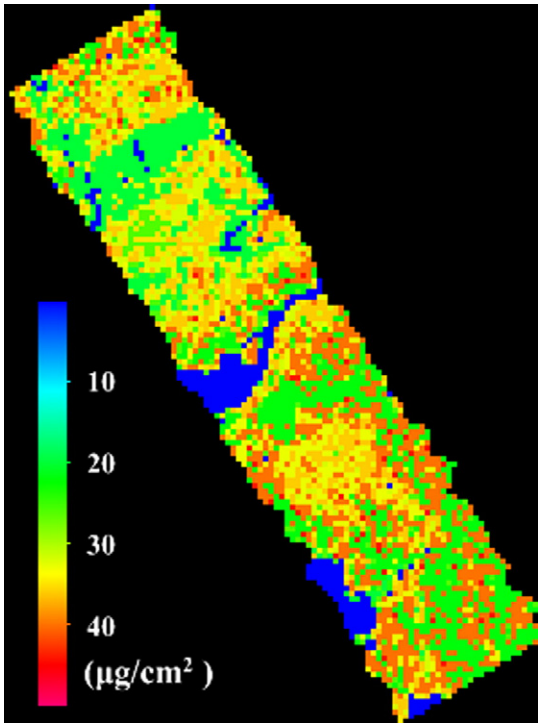

Plate II. CASI chlorophyll$_{a+b}$ content distribution per unit leaf area. The image is produced based on the retrieved chlorophyll$_{a+b}$ content for the three vegetated cover types. The spatial resolution of the image is 20×20 m.

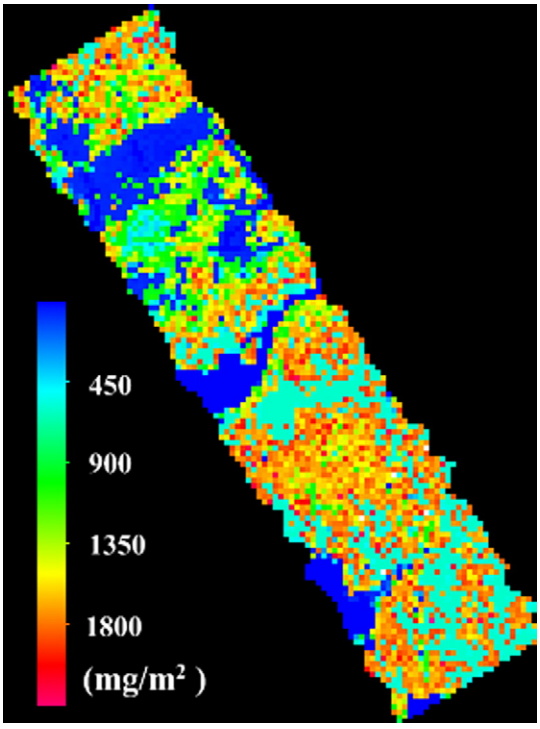

Plate III. CASI chlorophyll$_{a+b}$ content distribution per unit ground surface area. The image is derived based on the LAI image and retrieved chlorophyll$_{a+b}$ content per unit leaf area of the three vegetated cover types. The spatial resolution of the image is 20×20 m.

Stem density has the secondary importance in determining canopy reflectance. This study only developed LUTs as functions of LAI, and view and sun geometry. The assumption that the shaded reflectivities of tree crown and the background are comparatively small was made to reduce the unknown parameters in the model. The contribution of these two components was incorporated in the multiple scattering factor. In future studies, more comprehensive LUTs, which include LAI, sun and view geometry, stem density, and the two shaded components, can be generated to take into account the complexity of forests.

The probability of viewing forest background by the sensor is large in open forests. As the background compounds the effects of shadows, the BRDF correction to the measured background reflectance is necessary to account for the mutual shadowing effect among high understorey layers. In this study, the LUTs are developed under the assumption that forest background does not vary significantly across the landscape. Due to the heterogeneity and variability of forest background, the effects of forest background on the total remote sensing signals are uneven. To map chlorophyll content more accurately, the spatial variation of forest background needs to be estimated. Multi-angle remote sensing data have demonstrated the capability for deriving background reflectance (Canisius & Chen, 2007). With the retrieval of spatially explicit forest background reflectance, forest chlorophyll content mapping will be improved.

Detailed measurements of canopy architecture were not made, and general parameters were used as inputs to the model for the study sites. However, the 4-Scale model can be run with confidence as the model has been successfully demonstrated to be capable of (i) estimating the variability of forest background reflectance with a set of general parameters (Canisius & Chen, 2007), (ii) detecting forest structural change (Peddle et al., 2003), and (iii) estimating contributions of forest scene components across the wavelength spectrum (Chen et al., 1999). To map the chlorophyll content, this study used the reflectance and transmittance spectra of aspen leaves for deciduous species, and took the canopy reflectance of grass as leaf-level reflectance. In future studies, leaf optical properties and biochemical contents of deciduous and grass species need to be measured for validating the estimation and mapping chlorophyll accurately.

Forest chlorophyll content was mapped using a spatially coarsened LAI map. This scaling process is necessary as the canopy reflectance is estimated using the 4-Scale model, which assumes trees in a forest have certain patchiness and follow a Neyman distribution. If a pixel is too small, 1 pixel might not even cover a complete tree crown. To meet the conditions for this statistical tree distribution pattern, the canopy-to-leaf inversion algorithm is applied to coarsened pixels (20 m) in this study. Further algorithm development is yet needed to retrieve chlorophyll content at the original CASI resolution. This algorithm would have to avoid using any tree distribution assumptions. This is one of the remaining challenges that we have not yet tackled in this research.

6. Conclusion

In this study, we explore methods for retrieving leaf chlorophyll content from hyperspectral remote sensing measurements for complex forest canopies. A process-based approach is developed for retrieving leaf reflectance from hyperspectral remote sensing imagery, and thereby leaf chlorophyll content for both open and closed forests, which is in contrast to existing empirically based methods and some highly simplified methods for closed canopies. Our process-based approach produced systematically better estimates of chlorophyll$_{a+b}$ content than a widely used spectral index approach. The look-up-table approach developed in this study successfully separates the leaf optical properties and canopy structural effect, and links leaf-level optical properties to the canopy-level hyperspectral measurements. With the look-up tables, the effects of canopy structure and forest background are removed, and the geometrical–optical model 4-Scale was inverted to estimate leaf reflectance spectra from above-canopy remote sensing imagery. In combination with the leaf-level model PROSPECT, leaf chlorophyll content was estimated from the retrieved leaf reflectance, with an accuracy of R^2=0.47, RMSE=4.34 μg/cm^2, and a jackknifed RMSE=5.69 μg/cm^2 for the black spruce sites. Forest chlorophyll content was mapped based on the estimated leaf chlorophyll content and a retrieved leaf area index image. The mapped chlorophyll content at 20 m resolution can be useful for the assessment of forest growth and ecosystem health status.

Acknowledgments

The authors gratefully acknowledge the financial support of *GEOIDE* (Geomatics for Informed Decisions) part of the Networks of Centres of Excellence program and *NSERC* (Natural Sciences and Engineering Research Council of Canada), in-kind support provided through the Ontario Ministry of Natural Resources, and technical support from the Earth Observations Laboratory at York University, particularly Lawrence Gray and James Freemantle for CASI image acquisition and processing. We acknowledge Inian Moorthy of York University for the instructions on leaf spectral measurements and CASI image processing, technical assistance from Denny Irving, Lesley Rich, and Maara Packalen of the Ontario Forest Research Institute with the field sample collection and laboratory analyses of the foliage samples, and Mingzhen Chen and Gang Mo of the University of Toronto for their assistance on field and laboratory measurements. Sylvain Leblanc gave useful instructions on the use of the 4-Scale model and the processing of digital hemispherical photos. We thank Dr. Gina Mohammed for supplying the reflectance curve data for the Canada blue-joint grass. Finally, the comments of three anonymous reviewers helped to improve the final version of this paper.

References

Allen, W. A., Gausman, H. W., Richardson, A. J., & Thomas, J. R. (1969). Interaction of isotropic light with a compact plant leaf. *Journal of Optical Society of America*, *59* (10), 1376–1379.

Asner, G. P., Braswell, B. H., Schimel, D. S., & Wessman, C. A. (1998). Ecological research needs from multi-angle remote sensing data. *Remote Sensing of Environment*, *63*, 155–165.

Badhwar, G. D., MacDonald, R. B., & Mehta, N. C. (1986). Satellite derived leaf area index and vegetation maps as input to glocal carbon cycle models—A hierarchical approach. *International Journal of Remote Sensing*, *7*, 265–281.

Baret, F., Vanderbilt, V. C., Steven, M. D., & Jacquemoud, S. (1994). Use of spectral analogy to evaluate canopy reflectance sensitivity to leaf optical properties. *Remote Sensing of Environment*, *48*, 253–260.

Belanger, M. J., Miller, J. R., & Boyer, M. G. (1995). Comparative relationships between some red edge parameters and seasonal leaf chlorophyll concentrations. *Canadian Journal of Remote Sensing*, *21*, 16–21.

Borel, C. C., Gerstl, S. A. W., & Powers, B. J. (1991). The radiosity method in optical remote sensing of structured 3-D surfaces. *Remote Sensing of Environment*, *36*, 13–44.

Broge, N. H., & Leblanc, E. (2000). Comparing prediction power and stability of broadband and hyperspectral vegetation indices for estimation of green leaf area index and canopy chlorophyll density. *Remote Sensing of Environment*, *76*, 156–172.

Canisius, F., & Chen, J. M. (2007). Retrieving forest background reflectance in a Boreal region from Multi-angle Imaging SpectroRadiometer (MISR) data. *Remote Sensing of Environment*, *107*, 312–321.

Carter, G. A. (1994). Ratios of leaf reflectances in narrow wavebands as indicators of plant stress. *International Journal of Remote Sensing*, *15*, 697–704.

Chappelle, E. W., Kim, M. S., & McMurtrey, J. E. (1992). Ratio analysis of reflectance spectra (RARS): An algorithm for the remote estimation of the concentrations of chlorophyll *A*, chlorophyll B and the carotenoids in soybean leaves. *Remote Sensing of Environment*, *39*, 239–247.

Chen, J. M. (1996). Optically-based methods for measuring seasonal variation in leaf area index of boreal conifer forests. *Agricultural and Forest Meteorology*, *80*, 135–163.

Chen, J. M., & Cihlar, J. (1996). Retrieving leaf area index for boreal conifer forests using Landsat TM images. *Remote Sensing of Environment*, *55*, 153–162.

Chen, J. M., & Leblanc, S. (1997). A 4-scale bidirectional reflection model based on canopy architecture. *IEEE Transactions on Geoscience and Remote Sensing*, *35*, 1316–1337.

Chen, J. M., & Leblanc, S. G. (2001). Multiple-scattering scheme useful for hyperspectral geometrical optical modelling. *IEEE Transactions on Geoscience and Remote Sensing*, *39*(5), 1061–1071.

Chen, J. M., Leblanc, S. G., Miller, J. R., Freemantle, J., Loechel, S. E., Walthall, C. L., et al. (1999). Compact Airborne Spectrographic Imager (CASI) used for mapping biophysical parameters of Boreal forests. *Journal of Geophysical Research-Atmosphere*, *104*(D22), 27,945–27,948.

Chen, J. M., Menges, C. H., & Leblanc, S. G. (2005). Global mapping of foliage clumping index using multi-angular satellite data. *Remote Sensing of Environment*, *97*, 447–457.

Chen, J. M., Pavlic, G., Brown, L., Cihlar, J., Leblanc, S. G., White, H. P., et al. (2002). Validation of Canada-wide leaf area index maps using ground measurements and high and moderate resolution satellite imagery. *Remote Sensing of Environment*, *80*, 165–184.

Chen, J. M., Rich, P. M., Gower, T. S., Norman, J. M., & Plummer, S. (1997). Leaf area index of boreal forests: Theory, techniques and measurements. *Journal of Geophysical Research*, *102*, 29,429–29,444.

Curran, P. J. (1994). Imaging spectrometry. *Progress in Physical Geography*, *18*(2), 247–266.

Curran, P. J., Kupiec, J. A., & Smith, G. M. (1997). Remote sensing the biochemical composition of a slash pine canopy. *IEEE Transactions on Geosciences and Remote Sensing*, *35*, 415–420.

Dash, J., & Curran, P. J. (2004). The MERIS terrestrial chlorophyll index. *International Journal of Remote Sensing*, *25*, 5403–5413.

Datt, B. (1998). Remote sensing of chlorophyll a, chlorophyll b, chlorophyll *a* + *b* and total carotenoid content in eucalyptus leaves. *Remote Sensing of Environment*, *66*, 111–121.

Datt, B. (1999). A new reflectance index for remote sensing of chlorophyll content in higher plants: Tests using Eucalyptus leaves. *Journal of Plant Physiology*, *154*, 30–36.

Dawson, T. P., Curran, P. J., North, P. R. J., & Plummer, S. E. (1997). The potential for understanding the biochemical signal in the spectra of forest canopies using a coupled leaf and canopy model. In G. Guyot, & T. Phulpin (Eds.), *Physical measurements and signatures in remote sensing, Vol. 2*. (pp. 463–470)Rotterdam: Balkema.

Demarez, V., & Gastellu-Etchegorry, J. P. (2000). A modeling approach for studying forest chlorophyll content. *Remote Sensing of Environment*, *71*, 226–238.

Demarez, V., Gastellu-Etchegorry, J. P., Mougin, E., Marty, G., & Proisy, C. (1999). Seasonal variation of leaf chlorophyll content of a temperate forest. Inversion of the PROSPECT model. *International Journal of Remote Sensing*, *20*, 879–894.

Daughtry, C. S. T., Walthall, C. L., Kim, M. S., Brown, de C. E., & McMurtrey, J. E. (2000). Estimating corn leaf chlorophyll concentration from leaf and canopy reflectance. *Remote Sensing of Environment*, *74*, 229–239.

Davidson, D., Achal, S., Mah, S., Gauvin, R., Kerr, M., Tam, A., et al. (1999). Determination of tree species and tree stem densities in northern Ontario forests using airborne CASI data. *Proceedings of the Fourth International Airborne Conference and Exhibition, Ottawa, ON* (pp. 178–196)..

Fang, Z., Bouwkamp, J., & Solomos, T. (1998). Chlorophyllase activities and chlorophyll degradation during leaf senescence in nonyellowing mutant and wild type of *Phaseolus vulgaris* L. *Journal of Experimental Botany*, *49*, 503–510.

Ganapol, B., Johnson, L., Hammer, P., Hlavka, C., & Peterson, D. (1998). LEAFMOD: A new within-leaf radiative transfer model. *Remote Sensing of Environment*, *6*, 182–193.

Gastellu-Etchegorry, J. P., Demarez, V., Pinel, V., & Zagolski, F. (1996). Modelling radiative transfer in heterogeneous 3-D vegetation canopies. *Remote Sensing of Environment*, *58*, 131–156.

Gitelson, A. A., & Merzlyak, M. N. (1996). Signature analysis of leaf reflectance spectra: Algorithm development for remote sensing of chlorophyll. *Journal of Plant Physiology*, *148*, 494–500.

Gitelson, A. A., Merzlyak, M. N., & Lichtenthaler, H. K. (1996). Detection of red edge position and chlorophyll content by reflectance measurements near 700 nm. *Journal of Plant Physiology*, *148*, 501–508.

Goel, N. S., Rozehnal, I., & Thompson, R. L. (1991). A computer graphics based model for scattering from objects of arbitrary shapes in the optical region. *Remote Sensing of Environment*, *36*(2), 73–104.

Haboudane, D., Miller, J. R., Tremblay, N., Zarco-Tejada, P. J., & Dextraze, L. (2002). Integrated Narrow-Band Vegetation Indices for Prediction of Crop Chlorophyll Content for Application to Precision Agriculture. *Remote Sensing of Environment*, *81*, 416–426.

Hall, F. G., Shimabukuro, Y. E., & Huemmrich, K. F. (1995). Remote sensing of forest biophysical structure in boreal stands of *Picea mariana* using mixture decomposition and geometric reflectance models. *Ecological Applications*, *5*, 993–1013.

Harron, J. W., & Miller, J. R. (1995). An alternative methodology for reflectance and transmittance measurements of conifer needles. *17th Canadian Symposium on Remote Sensing, Saskatoon, Saskatchewan, II*. (pp. 654–661)Ottawa, Canada: Canadian Remote Sensing Society, Canadian Aeronautics and Space Institute.

Jacquemoud, S., & Baret, F. (1990). PROSPECT: A model of leaf optical properties spectra. *Remote Sensing of Environment*, *34*, 75–91.

Jacquemoud, S., Baret, F., Andrieu, B., Danson, F. M., & Jaggard, K. (1995). Extraction of vegetation biophysical parameters by inversion of the PROSPECT + SAIL models on sugar beet canopy reflectance data: Application to TM and AVIRIS sensors. *Remote Sensing of Environment*, *52*, 163–172.

Johnson, L. F., Hlavka, C. A., & Peterson, D. L. (1994). Multivariate analysis of AVIRIS data for canopy biochemical estimation along the Oregon transect. *Remote Sensing of Environment*, *47*, 216–230.

Latifovic, R., Cihlar, J., & Chen, J. M. (2003). A comparison of BRDF models for the normalization of satellite optical data to a standard sun-target-sensor geometry. *IEEE Transactions on Geoscience and Remote Sensing*, *41*(8), 1889–1998.

Lawrence, R., & Labus, M. (2003). Early detection of Douglas-fir beetle infestation with subcanopy resolution hyperspectral imagery. *Western Journal of Applied Forestry*, *18*, 202–206.

le Maire, G., Francois, C., & Dufrene, E. (2004). Towards universal broad leaf chlorophyll indices using PROSPECT simulated database and hyperspectral reflectance measurements. *Remote Sensing of Environment*, *89*, 1–28.

Leblanc, S. G., Bicheron, P., Chen, J. M., Leroy, M., & Cihlar, J. (1999). Investigation of bidirectional reflectance of boreal forests using airborne POLDER and the 4-scale model. *IEEE Transactions on Geoscience and Remote Sensing*, *37*, 1396–1414.

Lewis, M., Jooste, V., & de Gasparis, A. A. (2001). Discrimination of arid vegetation with airborne multispectral scanner hyperspectral imagery. *IEEE Transactions on Geoscience and Remote Sensing*, *39*, 1471–1479.

Li, X., & Strahler, A. H. (1988). Modeling the gap probability of discontinuous vegetation canopy. *IEEE Transactions on Geoscience and Remote Sensing*, *26*, 161–170.

Li, X., Strahler, A. H., & Woodcock, C. E. (1995). A hybrid geometric optical-radiative transfer approach for modeling albedo and directional reflectance of discontinuous canopies. *IEEE Transactions on Geoscience and Remote Sensing*, *33*, 466–480.

Liang, S., & Strahler, A. H. (1993). Calculation of the angular radiance distribution for a coupled atmosphere and canopy. *IEEE Transactions on Geoscience and Remote Sensing*, *31*(2), 491–502.

Luther, J. E., & Carroll, A. L. (1999). Development of an index of Balsam Fir vigor by foliar spectral reflectance. *Remote Sensing of Environment*, *69*, 241–252.

Matson, P., Johnson, L., Billow, C., Miller, J. R., & Pu, R. (1994). Seasonal patterns and remote spectral estimation of canopy chemistry across the Oregon transect. *Ecological Applications*, *4*, 280–298.

Miller, R. G., Jr. (1964). A trustworthy jackknife. *Annals of Mathematical Statistics*, *55*, 1594–1605.

Miller, R. G., Jr. (1968). Jackknifing variances. *Annals of Mathematical Statistics*, *39*, 52–567.

Mohammed, G. H., Noland, T. L., Irving, D., Sampson, P. H., Zarco-Tejada, P. J., & Miller, J. R., 2000. Natural and stress-induced effects on leaf spectral reflectance in Ontario species. Ont. Min. of Nat. Res., Ont. For. Res. Inst., Sault Ste. Marie, ON. For. Res. Rep. No. 156: 34p.

Moorthy, I., et al. (in press). Estimating chlorophyll concentration in conifer needles with hyperspectral data: An assessment at the needle and canopy level, *Remote Sensing of Environment*, doi:10.1016/j.rse.2008.01.013

Myneni, R., Asrar, G., & Gerstl, S. (1990). Radiative transfer in three dimensional leaf canopies. *Transport Theory and Statistical Physics*, *19*, 205–250.

Nemani, R. R., Pierce, L. L., Running, S. W., & Band, L. (1993). Forest ecosystem processes at the watershed scale: Sensitivity to remotely sensed leaf area index estimates. *International Journal of Remote Sensing*, *14*(13), 2519–2534.

Noland, T. L., Miller, J. R., Moorthy, I., Panigada, C., Zarco-Tejada, P. J., Mohammed, G. H., et al., 2003. Bioindicators of forest sustainability: Using remote sensing to monitor forest condition. In: Meeting emerging ecological, economic, and social challenges in the Great Lakes region: Popular summaries. Compiled by L.J. Buse and A.H. Perera, Ontario Forest Research Institute, Ontario Ministry of Natural Resources, Forest Research Information 155: 75–77.

O ' Neill, N. T., Zagolski, F., Bergeron, M., Royer, A., Miller, J. R., & Freemantal, J. (1997). Atmospheric correction validation of CASI images acquired over the BOREAS southern study area. *Canadian Journal of Remote Sensing*, *23*, 143–162.

Peddle, D. R., Franklin, S. E., Johnson, R. L., Lavigne, M. A., & Wulder, M. A. (2003). Structural change detection in a disturbed conifer forest using a geometric optical reflectance model in multiple-forward mode. *IEEE Transactions on Geoscience and Remote Sensing*, *41*(1), 163–166.

Peñuelas, J., Baret, F., & Filella, I. (1995). Semiempirical indices to assess carotenoids chlorophyll: A ratio from leaf spectral reflectance. *Photosynthetica*, *31*, 221–230.

Peterson, D. L., Aber, J. D., Matson, P. A., Card, D. H., Swanberg, N. A., Wessman, C. A., et al. (1988). Remote sensing of forest canopy leaf biochemical contents. *Remote Sensing of Environment*, *24*, 85–108.

Peterson, D. L., Spanner, M. A., Running, S. W., & Teuber, K. B. (1987). Relationship of thematic mapper simulator data to leaf area index of temperate coniferous forests. *Remote Sensing of Environment*, *22*, 323–341.

Pragnère, A., Baret, F., Weiss, M., Myneni, R. B., Knyazikhin, Y., & Wang, L. B. (1999). Comparison of three radiative transfer model inversion techniques to estimate canopy biophysical variables from remote sensing data. *Proceedings of the International Geoscience and Remote Sensing Symposium (IGARSS'99), June 28–July 2, Hamburg, Germany*.

Renzullo, L. J., Blanchfield, A. L., Guillermin, R., Powell, K. S., & Held, A. A. (2006). Comparison of PROSPECT and HPLC estimates of leaf chlorophyll contents in a grapevine stress study. *International Journal of Remote Sensing*, *27*(4), 817–823.

Rock, B. N., Hoshizaki, T., & Miller, J. R. (1988). Comparison of in situ and airborne spectral measurements of the blue shift associated with forest decline. *Remote Sensing of Environment*, *24*, 109–127.

Sampson, P. H., Zarco-Tejada, P. J., Mohammed, G. H., Miller, J. R., & Noland, T. L. (2003). Hyperspectral remote sensing of forest condition: Estimating chlorophyll content in tolerant hardwoods. *Forest Science*, *49*(3), 381–391.

Sims, D. A., & Gamon, J. A. (2002). Relationships between leaf pigment content and spectral reflectance across a wide range of species, leaf structures and developmental stages. *Remote Sensing of Environment*, *81*, 337–354.

Thompson, R. L., & Goel, N. S. (1999). SPRINT: A universal canopy reflectance model for kilometer level scene. *Abstract of the Second International Workshop on Multiple-Angle Measurements and Models, Sept. 15–17, Ispra, Italy*.

Verhoef, W. (1984). Light scattering by leaf layers with application to canopy reflectance modelling: The SAIL model. *Remote Sensing of Environment*, *16*, 125–141.

Verstaete, M. M., Pinty, B., & Dickinson, R. E. (1990). A physical model of the bidirectional reflectance vegetation canopies, I Theory. *Journal of Geophysics Research*, *95*(D8), 11,755–11,765.

Yoder, B. J., & Pettigrew-Crosby, R. E. (1995). Predicting nitrogen and chlorophyll content and concentrations from reflectance spectra (400–2500 nm) at leaf and canopy scales. *Remote Sensing of Environment*, *53*(3), 199–211.

Zagolski, F., Pinel, V., Romier, J., Alcayde, D., Fotanari, J., Gastellu-Etchegorry, J. P., et al. (1996). Forest canopy chemistry with high spectral resolution remote sensing. *International Journal of Remote Sensing*, *17*, 1107–1128.

Zarco-Tejada, P.J., 2000. Hyperspectral remote sensing of closed forest canopies: Estimation of chlorophyll fluorescence and pigment content. Ph.D thesis, York University, Toronto, ON, Canada.

Zarco-Tejada, P. J., & Miller, J. R. (1999). Land cover mapping at BOREAS using red edge spectral parameters from CASI imagery. *Journal of Geophysics Research*, *104*(D22), 27921–27948.

Zarco-Tejada, P. J., Berjón, A., López-Lozano, R., Miller, J. R., Martín, P., Cachorro, V., et al. (2005). Assessing vineyard condition with hyperspectral indices: Leaf and canopy reflectance simulation in a row-structured discontinuous canopy. *Remote Sensing of Environment*, *99*, 271–287.

Zarco-Tejada, P. J., Miller, J. R., Harron, J., Hu, B., Noland, T. L., Goel, N., et al. (2004a). Needle chlorophyll content estimation through model inversion using hyperspectral data from boreal conifer forest canopies. *Remote Sensing of Environment*, *89*, 189–199.

Zarco-Tejada, P. J., Miller, J. R., Morales, A., Berjón, A., & Agüera, J. (2004b). Hyperspectral indices and model simulation for chlorophyll estimation in open-canopy tree crops. *Remote Sensing of Environment*, *90*(4), 463–476.

Zarco-Tejada, P. J., Miller, J. R., Noland, T. L., Mohammed, G. H., & Sampson, P. H. (2001). Scaling-up and model inversion methods with narrow-band optical indices for chlorophyll content estimation in closed forest canopies with hyperspectral data. *IEEE Transactions on Geosciences and Remote Sensing*, *39*(7), 1491–1507.

Zhang, Y., Chen, J. M., Miller, J. R., & Noland, T. L., 2008 (in revision). Retrieving chlorophyll content of conifer needles from hyperspectral measurements. *Canadian Journal of Remote Sensing*

Zhang, Y., Chen, J. M., & Miller, J. R. (2005). Determining digital hemispherical photograph exposure for leaf area index estimation. *Agricultural and Forest Meteorology*, *133*, 166–181.

Zhang, Y., Chen, J. M., & Thomas, S. C. (2007). Retrieving seasonal variation in chlorophyll content of overstorey and understorey sugar maple leaves from leaf-level hyperspectral data. *Canadian Journal of Remote Sensing*, *5*, 406–415.